

Theory of stripes in quasi two dimensional rare-earth tellurides

Hong Yao, John A. Robertson, Eun-Ah Kim, and Steven A. Kivelson
 Department of Physics, Stanford University, Stanford, CA 94305
 (Dated: March 23, 2002)

Even though the rare-earth tritellurides are tetragonal materials with a quasi two dimensional (2D) band structure, they have a "hidden" 1D character. The resultant near-perfect nesting of the Fermi surface leads to the formation of a charge density wave (CDW) state. We show that for this band structure, there are two possible ordered phases: A bidirectional "checkerboard" state would occur if the CDW transition temperature were sufficiently low, whereas a unidirectional "striped" state, consistent with what is observed in experiment, is favored when the transition temperature is higher. This result may also give some insight into why, in more strongly correlated systems, such as the cuprates and nickelates, the observed charge ordered states are generally stripes as opposed to checkerboards.

I. INTRODUCTION

Many strongly correlated (layered) materials with quasi two dimensional (2D) structure show fluctuating or static stripe order (unidirectional density wave states) over a substantial range of temperatures.^{1,2,3} In particular, there has been considerable interest in studying whether or not stripes are inextricably connected to the high temperature superconductivity that occurs in the cuprates.^{1,2} However, characterizing the stripe order in these materials is difficult due to the complex and strongly correlated nature of these materials, and the presence of significant amounts of quenched disorder.⁴

From the symmetry view point, there is no difference between a unidirectional charge density wave state (CDW) in a weakly interacting quasi-2D system and a stripe-ordered state of a strongly correlated system. CDW states can occur in the weak coupling limit only if there are sufficiently well nested portions of the Fermi surface. Since this is non-generic in more than 1D, one would like to identify what is special about those higher dimensional materials in which nested Fermi surfaces appear. Moreover, for a layered quasi-2D material with tetragonal (C_4) symmetry, the CDW ground state can either be bidirectional (checkerboards) maintaining the point group symmetry of the lattice, or unidirectional (stripes) with a reduced symmetry, and again we would like to understand what physics governs this choice.

The rare-earth tritelluride series RTe_3 ($R = Y, La-Tm$) is particularly well suited for a detailed study of these issues. RTe_3 consists of square Te planes alternating with weakly coupled RTe slabs. (See Fig. 2 of Ref. 5 for example.) The electronically active valence band derives from the 5p orbitals of the planar Te atoms, and is thus expected to be relatively weakly correlated. The existence of a unidirectional CDW was first detected by transmission electron microscopy (TEM).^{6,7} Angle resolved photoemission spectroscopy (ARPES)^{5,8,9} measurements have shown that the CDW ordering wavevector nests large portions of the Fermi surface, which are in turn gapped, thus strongly indicating that the CDW is a consequence of Fermi surface nesting. More recent X-ray scattering and STM measurements have confirmed the

existence of the CDW and its unidirectional character in great detail.^{10,11} Detailed studies of the Fermi surface topology using ARPES⁵ and positron annihilation¹² support the notion that the CDW is the result of a nesting-driven Fermi surface instability. However, the driving force for the strong breaking of the point group symmetry ($C_4 \rightarrow C_2$) produced by the unidirectional CDW formation in RTe_3 has not been clear previously.

We shall show in the present paper that the nesting of the Fermi surface of RTe_3 reflects a "hidden" 1D character of the electronic band structure which derives from the highly anisotropic hopping amplitude of the Te p_x and p_y orbitals.¹³ Consequently, CDW order occurs for a dimensionless effective interaction, U_c , in excess of an extremely small critical value, $U_{c0} \approx 1$. (In 1D, the fact that $U_{c0} = 0$ is the famous Peierls instability.) Moreover, we shall show that there are two possible patterns of CDW order that can take best advantage of the nesting: checkerboard order that occurs for U_c slightly larger than U_{c0} , and stripe order, which is also rotated relative to the checkerboard order, which occurs for $U_c > U_{c0} [1 + O(U_{c0})]$; in more physical terms, what this means is that when the CDW transition temperature, T_c , or the CDW gap, Δ_0 , is sufficiently large, stripe order is favored. (The resulting phase diagram is shown in Fig. 4.)

II. BAND STRUCTURE CONSIDERATIONS

It is well established from transport measurements^{14,15} that the coupling between layers in RTe_3 is small. Comparisons between different rare earth compounds confirm the minor role of the rare earth in the electronic structure.^{5,15} Hence the physical properties of RTe_3 are dominantly determined by the Te planes common to all RTe_3 . It is therefore natural to consider a simple model of the electronic structure of a single Te plane.

It is known, from first principle band structure calculations,¹⁶ that the energy of the 5p_z is shifted by crystal field effects so that it lies well below the Fermi energy. Consequently, the relevant bands close to the Fermi surface are the 5p_x and 5p_y orbitals, which are

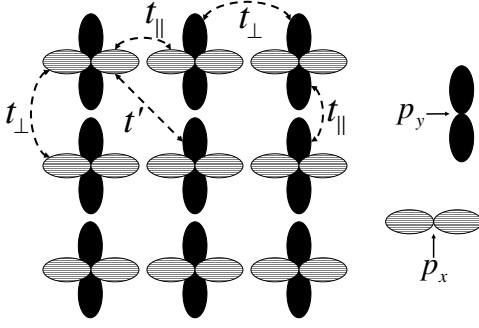


FIG. 1: The p_x (hatched) and p_y (solid) orbitals in the single Te square lattice. Due to the highly anisotropic profile of the p orbitals, the hopping amplitude, t_k , along the extended direction of the given p orbital is much larger than the hopping amplitude t_\perp along the direction perpendicular to the extended direction. t^0 is a second-neighbor hopping, which is the shortest-range interaction which mixes the p_x and p_y bands, and which we neglect for present purposes.

approximately 5/8 filled. The crystallographic unit cell contains two Te atoms per plane due to a slight inequivalence between two sublattices produced by the RTe slab orientation and the crystal structure is very weakly orthorhombic;^{1,2} for simplicity, we will ignore these subtleties and consider an idealized Te square lattice. The band structure can be well approximated in the tight-binding approximation; the resulting Hamiltonian is shown schematically in Fig. 1.

Following Ref. 6, we neglect all interactions of longer-range than the nearest neighbor hopping, with the consequence that there is no hybridization between the p_x and p_y bands. (Small further neighbor interactions, such as the second neighbor hopping t^0 in Fig. 1, have a large effect on the Fermi surface topology where the two bands intersect, but can readily be shown to have little effect on the results obtained below.) Working in units where the lattice constant of the square lattice $a = 1$, the dispersion for the p_x band and p_y band can be readily derived:

$$\begin{aligned} \epsilon_{p_x} &= 2t_k \cos(k_x) + 2t_\perp \cos(k_y) \\ \epsilon_{p_y} &= 2t_\perp \cos(k_x) - 2t_k \cos(k_y); \end{aligned} \quad (2.1)$$

where t_k (t_\perp) represents the hopping amplitude parallel (perpendicular) to the extended direction of the given p orbital. Due to the highly anisotropic profile of the p orbital electron wave function, the hopping amplitude t_k , along the extended direction of the given p orbital, is much larger than the hopping amplitude t_\perp perpendicular to the extended direction. Indeed these hopping amplitudes have been estimated¹⁶ to be $t_k \approx 2.0\text{eV}$, $t_\perp \approx 0.37\text{eV}$, and $t^0 \approx 0.16\text{eV}$ for RTe. Thus, it is reasonable to set $t^0 = 0$ and to treat $t_\perp = t_k \approx 0.18$ as a small parameter.

The small magnitude of the ratio $t_\perp = t_k$ implies a secret quasi-1D character of the band structure. For $t_\perp = 0$, the system would be equivalent to an array of 1D wires.

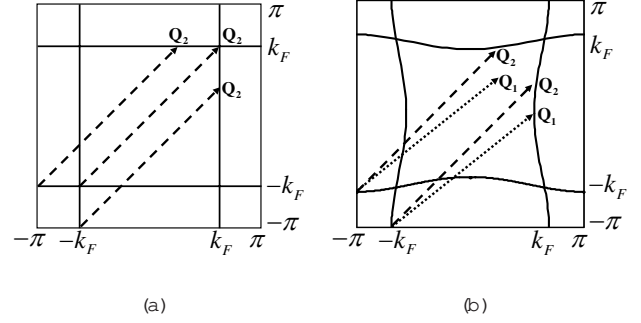


FIG. 2: Fermi surfaces (a) for $t_\perp = 0$ and (b) for t_\perp small, but non-zero. For $t_\perp = 0$, the wavevector $Q_2 = (2k_F; 2k_F)$ nests both the p_x -FS and the p_y -FS perfectly. For non-zero t_\perp , the wavevector $Q_1 = (2k_F; 0)$ does a much better job of nesting the p_x -FS but a poor job on the p_y -FS. On the other hand, Q_2 does a moderately good job of nesting the entire FS.

Nonetheless, the system would maintain overall C_4 symmetry since these p_x and p_y "wires" are perpendicular to each other. Thus, even in this limit, the system would not display 2D anisotropy in any transport measurement. However, the resulting band structure would consist of two parallel 1D FS's as shown in Fig. 2(a). With k_F defined by the implicit relation $\epsilon_F = 2t_k \cos k_F$, where ϵ_F is the chemical potential, any wavevector $(2k_F; k_y)$ would then perfectly nest the p_x -FS for arbitrary k_y and wavevectors $(k_x; 2k_F)$ would perfectly nest the p_y -FS for any k_x . In particular, the wavevectors $(2k_F; 2k_F)$ perfectly nest both the p_x and p_y FS's.

A small, but nonzero t_\perp introduces nonzero but small curvature to the FS (see Fig. 2(b)); the p_x -FS is determined by

$$k_x = k_F + \frac{t_\perp}{t_k} \frac{\cos k_y}{\sin k_F} + O\left(\frac{t_\perp^2}{t_k^2}\right); \quad (2.2)$$

where k_F is defined above. Here $+$ ($-$) represents the right (left) portion of the p_x -FS respectively. Obviously, the p_y -FS can be obtained from the p_x -FS by 90° rotation.

As a consequence of the finite curvature, the wavevector $(2k_F; k_y)$ nearly perfectly nests the p_x -FS only for $k_y = 0$, and equivalently the p_y -FS is best nested by $(k_x; 2k_F)$. However, away from the half filling, $(2k_F; 0)$ does a poor job in nesting the p_y -FS and conversely for $(0; 2k_F)$. Note that $(2k_F; 0)$, $(0; 2k_F)$, $(2k_F; 2k_F)$ and $(-2k_F; -2k_F)$ are related by the C_4 symmetry of the host lattice. On the other hand, the wavevector $(2k_F; 2k_F)$ (and its C_4 symmetry related vectors), which perfectly nests the full FS for $t_\perp = 0$, does a reasonable job in nesting both the p_x -FS and the p_y -FS. Thus, for small $t_\perp = t_k$, there are two independent candidates (not related to each other via C_4 symmetry) for the CDW ordering

wavevectors:

$$Q_1 = (2k_F; 0) \quad \text{and} \quad Q_2 = (2k_F; 2k_F): \quad (2.3)$$

To see which ordering vector is preferred, we now compute the corresponding charge density (Lindhard) susceptibility, $\chi(q; T)$. For a given wavevector q at a given temperature T ,

$$\chi(q; T) = \frac{1}{2} \sum_{\mathbf{k}} \int_{-\infty}^{\infty} \frac{dk}{(2\pi)^2} \frac{f(k; T) - f(k+q; T)}{k - k+q}; \quad (2.4)$$

where the integral is over the first Brillouin zone, $\mathbf{k} = k_x; k_y$ is the band index, and $k = |\mathbf{k}|$. The factor of 2 is from two spin polarizations of the electrons and $f(k; T)$ denotes the Fermi-Dirac distribution function.

For small $t_F = t_k$, the susceptibilities at these two vectors have the following approximate analytical forms, which are valid for temperatures $T \ll t_F$ (in units $k_B = 1$):

$$\chi(Q_1; T) = (E_F) \log \frac{t_k}{T + t_F^2} + (E_F) \log \frac{t_k}{T + t_F^2}; \quad (2.5)$$

$$\chi(Q_2; T) = 2(E_F) \log \frac{t_k}{T + t_F^2}; \quad (2.6)$$

where $(E_F) = [2k_F \sin k_F]^{-1}$ is the density of states per spin per band and t_k is the ultraviolet cutoff, which is of order of the bandwidth (~ 2). The parameters t_i are defined by

$$\begin{aligned} 1 &= j \cos k_F = 4 \sin^2 k_F; \\ 2 &= 2j \cos k_F; \\ 3 &= j \cos k_F; \end{aligned} \quad (2.7)$$

In RTe_3 , the bands are approximately $5/8$ filled, thus $k_F = 5/8\pi$. In the small but non-zero $t_F = t_k$ limit,

$$\chi(Q_1; 0) = \chi(Q_2; 0) + (E_F) \log [2 \sin^2(k_F)]: \quad (2.8)$$

Therefore, if the CDW transition occurs at low enough temperatures the wavevector Q_1 will be favored so long as $\sin^2 k_F > 3/4$. However, at high enough temperatures, $T > T_0$ ($t_F = t_k$), $\chi(Q_2; T)$ is greater than

$\chi(Q_1; T)$. Therefore, we expect there to be a finite temperature T_0 such that if the CDW transition temperature $T_c < T_0$, the ordering vector is $q = Q_1$, while for $T_c > T_0$, $q = Q_2$.

For a more quantitative analysis, we have numerically evaluated the susceptibility $\chi(q; T)$ of Eq. (2.4), for wavevectors q over the whole Brillouin zone. The calculated susceptibility has a maximum at a wavevector q_{max} close to Q_1 or Q_2 , depending on whether the temperature, $T < T_0$ or $T > T_0$, in agreement with our analysis of the FS. The precise location of q_{max} shifts slightly as a function of T , but so long as $T \ll t_k$, the maximum

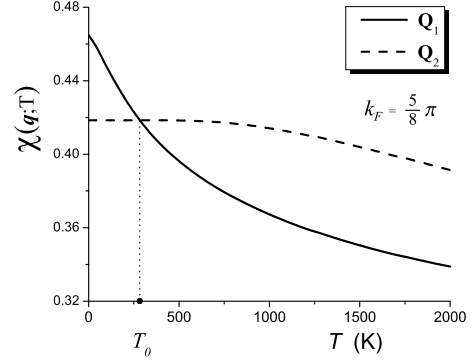


FIG. 3: The Lindhard susceptibility $\chi(q; T)$ as a function of T for $q = Q_1 = (2k_F; 0)$ and $q = Q_2 = (2k_F; 2k_F)$.

always lies close to Q_j , so this deviation does not significantly affect the resulting picture of the phase diagram. We will henceforth neglect this small effect, and focus our discussion on the wavevectors Q_j . Fig. 3 shows the calculated $\chi(q; T)$ for $q = Q_j$.

This result can be understood as follows: At low temperatures, the states arbitrarily close to the nearly perfectly nested portions of the Fermi surface dominate the susceptibility favoring Q_1 . However, for $T > T_0$, the curvature of the FS has negligible effect, so Q_2 is preferred. Since Q_1 nests only the p_x portion of the FS, there is little competition between the ordering tendency at Q_1 and at the symmetry related vector, $Q_1 = (0; 2k_F)$. Thus, as we shall show below, wherever CDW ordering with wavevector Q_1 occurs, simultaneous ordering occurs at $Q_1 = (0; 2k_F)$, making this a state with "checkerboard" order. However, since ordering at wavevector Q_2 opens a gap on the entire FS, it prevents ordering at the symmetry related vector, $Q_2 = (2k_F; 2k_F)$; when Q_2 is the preferred ordering vector, the resulting state has "stripe" order.

III. MEAN-FIELD PHASE DIAGRAM

To obtain an explicit phase diagram, we add an electron-phonon coupling and solve the resulting model in mean-field approximation. Thus, we investigate the following mean-field Hamiltonian

$$H_{MF} = \sum_{\mathbf{k}} \sum_{\sigma} c_{\mathbf{k}\sigma}^\dagger c_{\mathbf{k}\sigma} + \sum_{\mathbf{q}} \frac{(E_F)}{2} \sum_{\sigma} j_{\mathbf{q}} c_{\mathbf{k}\sigma}^\dagger c_{\mathbf{k}+\mathbf{q}\sigma} + \sum_{\mathbf{k}; \mathbf{q}} c_{\mathbf{k}\sigma}^\dagger c_{\mathbf{k}+\mathbf{q}\sigma}; \quad (3.1)$$

where the sum over q runs over the possible ordering vectors, $q = Q_1; Q_2$ and $Q_2; Q_1$, and all harmonics, such as $2Q_j$ and $Q_j - Q_j$. The order parameter q for the CDW with the ordering vector q is related to

from stripe order is $t_0 = 0.103$; the tricritical coupling is $t_{tc} = 0.105$; the temperature at the tricritical point is $T_{tc} = 0.098$ eV. The maximum checkerboard ordering temperature, T_0 , which occurs on the edge of the first order transition to the striped phase, is the one qualitative feature of the phase diagram that depends on the higher order terms in the Landau expansion that we have not computed. The estimate for T_0 given in the figure comes from the assumption that the first order phase boundary lies close to the point at which r_2 vanishes.

IV. FLUCTUATION EFFECTS

Because of the hidden 1D character of the ordering we have been exploring, we expect fluctuation effects will have a large quantitative effect on the mean-field phase diagram. Indeed, it is common in quasi 1D CDW systems for the ordering temperature, T_c to be significantly suppressed below its mean-field value. This is reflected in larger values (than the prediction of mean-field theory) of the ratio, t_0/T_c , of the zero temperature gap to the actual T_c .^{17,18}

We can estimate the extent to which fluctuations suppress T_c in two different limits: If the anisotropy is not too large, i.e. if $t_k \ll t_2 \ll 0$, the suppression is fractionally small, and can be estimated, as in the theory of superconductivity, by the Brout criterion, $T_{MF} - T_c \approx T_{MF}^2/t_k t_2$. Conversely, if $t_k \ll 0 \ll t_2$, while t_0 may still be crudely determined by mean-field considerations, $T_c \approx T_{MF}$ and is determined by entirely different physics. In this limit, the intra-chain CDW fluctuations can be treated using the theory of the one dimensional electron gas, and t_2 can be included in the context of inter-chain mean-field theory, with the result that $T_c \approx t_2/t_k$ where t_2 is an interaction dependent constant.^{19,20} Whenever there is a large fluctuational suppression of T_c , local CDW correlations are expected to survive in a broad range of temperatures above T_c ; roughly, the local CDW correlations develop in the temperature range $T_c < T < T_{MF}$, where T_{MF} is the mean-field transition temperature.

For $R\text{Te}_3$, $t_0 \approx 260 - 400$ meV⁵, corresponding to a mean transition temperature $T_{MF} \approx 1500 - 2000$ K and $t_0 \approx 0.1$. Since $t_k \approx 0.38$ eV ≈ 0 , a reliable estimate of T_c is not possible for these materials, although a large suppression relative to the mean-field value can be expected. An expression due to Barisic²¹ based on physically plausible but hard to justify approximations yields $T_c \approx (t_2/t_k)T_{MF} \approx 300$ K. Indeed, very recently, it has been found²² that the CDW phase transition in $R\text{Te}_3$ occurs (depending on R) in the range $T_c = 260 - 400$ K, and substantial CDW correlations persist well above T_c .

One consequence of remaining local CDW correlations above T_c will be the presence of peaks in the structure factor at positions corresponding to the Bragg vectors of the ordered state, but with width inversely proportional to the thermal correlation length.²³ However in

the case of a stripe phase, more dramatic effects can be expected. If there is only a single transition; then the "stripe liquid" phase above T_c does not break any of the lattice symmetries, and consequently equivalent peaks in the structure factor should appear both at the stripe ordering vector, and at the conjugate wavevector (rotated by 90°). Such behavior has already been seen, albeit only in the magnetic scattering, in the stripe liquid phase of $\text{La}_{2-x}\text{Sr}_x\text{NiO}_4$.²⁴ On the other hand, a two stage transition is also possible with an intermediate, "stripe nematic" phase,²⁵ in which stripe fluctuations are sufficiently violent to restore translation, but not the full C_4 symmetry of the host crystal; in such a phase, the peaks at the stripe ordering wave vector should be stronger (possibly, much stronger) than those at the conjugate wavevector. In this case, there must be a second transition at still higher temperatures to an isotropic state.

If future experiments can confirm the predictions above regarding the fluctuation effect, they will provide an important laboratory for exploring the physics of a stripe liquid, with possible broader implications to many striped materials.

V. CONCLUDING REMARKS

The present mean-field theory gives results that are broadly consistent with experimental observations in $R\text{Te}_3$. From the value of the CDW gap measured by ARPES,^{5,8} one can estimate the mean-field transition temperature to be $T_{MF} \approx 2000$ K, which is an order of magnitude greater than the theoretical value of T_0 and also greater than T_{tc} . Hence, the theory predicts that $R\text{Te}_3$ should have a unidirectional CDW ordered phase (stripes) with ordering vector approximately equal to either $Q_2 = (2k_F; 2k_F)$ or $Q_2 = (2k_F; -2k_F)$.²⁶ This is consistent with the experiments^{5,6,8} which find stripe order with $Q_{CDW} = (0.71; 0.71)$ in the present non-doubled unit cell notation.²⁷ With the simplified band-structure used in the present analysis, $2k_F \approx 3/4 \pmod{2}$. However, as mentioned above, the maximum of the susceptibility occurs at a slightly different weakly temperature dependent wave-vector; at $T = 350$ K, the maximum occurs at $q_{max} = (0.72; 0.72)$, which is almost identical to the experimental results at comparable temperatures. Moreover, the mean-field theory predicts that the phase transition into the stripe ordered phase from higher temperature phase is a second order phase transition. This is also consistent with recent experimental results.²²

Even though we are dealing with a stoichiometric phase with an integer number of electrons per unit cell, if the transition is continuous, then (at least for commensurability $N > 4$) the CDW ordered state just below T_c is generically incommensurate, in the sense that the ordering vector is not locked to the lattice. This follows from the fact that the lowest order term which locks the CDW to the lattice is proportional to $N^{-1} \cos(N\theta)$ and so is ir-

relevant (for $N > 4$) in the renormalization group sense²⁸ at T_c . (Here ξ is the order parameter and $\xi = 2k_F x_0$ determines the relative phase between the CDW and the underlying crystalline lattice.) In the present problem, two effects contribute to shift the ordering vector from its commensurate value. Firstly, even at $T = 0$, there is a shift of $k_F = 3/4[1 + O(t_b/t_k)^2]$ (which we have not discussed explicitly) due to the 2D dispersion. Moreover, Q_2 depends weakly on the temperature and (as mentioned above) is noticeably different from its $T = 0$ value at $T = T_c$. However, it is possible that, under appropriate circumstances, there will be a second commensurability lock-in transition with critical temperature $T_{com} < T_c$.

Another subtlety of the problem derives from the existence of Te bilayers in $R\text{Te}_3$. If the bilayer splitting, $t_{bil} \rightarrow 0$, it can be ignored, and a single transition occurs as treated in the present work. However, if $t_k \rightarrow t_{bil} \rightarrow 0$, we should treat the ordering in the bilayer split bands separately. In this case, there should be two distinct ordering transitions, at distinct ordering temperatures, with slightly different ordering vectors, $k_F = k_F$, $t_{bil} = v_F$.

Recent results²² on $R\text{Te}_3$ with different rare earth elements, R , show that in some cases there does, in fact, appear to be a second phase transition at temperatures below T_c . For various reasons, we conjecture that where the second transition occurs, it is due to the bilayer splitting, but whether it is this, or a commensurate lock-in, or some other transition remains unsettled.

Charge density waves often break the point group symmetry of the host lattice. This phenomenon is particularly common in strongly correlated materials including many transition metal oxides which exhibit stripe order. The strong interactions present in those (d-band) systems make the physics of pattern selection more difficult to study from a microscopic viewpoint. However, one may hope that extrapolating from the weak coupling limit (solved in the present paper) may give some insight into the deeper issues of pattern selection in highly correlated materials.

The underlying physics that is responsible for the existence of a CDW state in the present class of reasonably weakly interacting quasi-2D systems is the existence of a hidden 1D character of the band structure. In the present paper, we have explored only the grossest aspects of this structure – primarily those amenable to a mean-field analysis. At temperatures or frequencies in excess of the ordering temperature, where the band structure can be approximated as that of intersecting 1D systems, it is probable that more interesting fluctuation effects, associated with the breakdown of Fermi liquid theory in 1D, should be observable. Indeed, some evidence already exists²⁹ from high energy spectroscopies of anomalous power-law behaviors reminiscent of the 1D Luttinger liquid. We are currently exploring this aspect of the problem.

Acknowledgments We would like to thank S. Brown, A. Fang, I. R. Fisher, A. Kapitulnik, N. Ru and K. Y. Shin, for helpful discussions, and J. Allen and G. H. Gweon for partially inspiring this work. This work was supported in part by NSF grant number DMR 0531196 at Stanford University.

APPENDIX A: THE LINKED CLUSTER EXPANSION

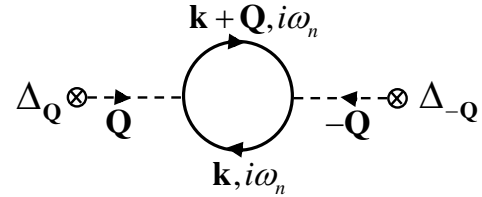


FIG. 5: The second order Feynman diagram from which we obtain the Lindhard susceptibility, χ_Q . Higher order diagrams differ only in the number of external legs.

Here we sketch the details of the linked cluster expansion that was used to obtain the coefficients of the GL free energy. We treat the off-diagonal part of the mean field Hamiltonian Eq. (3.1)

$$V = \sum_{k,q} \sum_{\alpha} c_{k+q}^{\alpha} c_k^{\alpha} \quad (\text{A } 1)$$

as a perturbation to obtain the Landau free energy:

$$F[f_q, g] = F_0 + \sum_q \frac{(E_F)}{2} j_q^2 + \sum_{l=2}^{\infty} U_l[f_q, g]; \quad (\text{A } 2)$$

where the set f_q, g contains, in principle, all harmonics of the fundamental ordering vectors, although in practice we restrict ourselves to fourth order terms for the continuous phase transitions. The functionals, U_l , are defined as

$$U_l = \frac{(1)^{l+1}}{l!} \frac{1}{Z} \int \prod_{\alpha} d\alpha_{\alpha} \int \prod_{\alpha} d\alpha_{\alpha} \exp(-V(\alpha)) \quad (\text{A } 3)$$

The expansion in terms of U_l contains only fully connected, 1-loop diagrams, where the finite-temperature Green functions for the electrons are

$$G_0(k; i\omega_n) = \frac{1}{i\omega_n - \epsilon_k}; \quad (\text{A } 4)$$

with $\epsilon_n = (2n + 1)\pi$, and the order parameters, Q_1, Q_2 , act as external, single-particle potentials (see, for example, Fig. 5).

To fourth order, the Landau free energy in terms of order parameters associated with Q_1, Q_2 and their harmonics is

$$F = F_0 + \sum_{j=1}^{X^2 n} r_j (j_{Q_j}^2 + j_{Q_j}^2) + r_j (j_{2Q_j}^2 + j_{2Q_j}^2) + r_j (j_{Q_j+Q_j}^2 + j_{Q_j-Q_j}^2) + d_j (j_{Q_j}^4 + j_{Q_j}^4) + g_j j_{Q_1}^2 j_{Q_2}^2 + b_j \left(\frac{2}{Q_j} \frac{2}{Q_j} + \frac{2}{Q_j} \frac{2}{Q_j} \right) + c_j \left(\frac{2}{Q_j} \frac{2}{Q_j} \frac{2}{Q_j} \frac{2}{Q_j} + \frac{2}{Q_j} \frac{2}{Q_j} \frac{2}{Q_j} \frac{2}{Q_j} \right) + c.c.]^0; \quad (A 5)$$

where the coefficients are given by the integrals

$$r_j = \langle E_F \rangle = \langle Q_j; T \rangle \quad (A 6)$$

$$r_j = \langle E_F \rangle = \langle 2Q_j; T \rangle \quad (A 7)$$

$$r_j = \langle E_F \rangle = \langle Q_j + Q_j; T \rangle \quad (A 8)$$

$$b_j = \int_0^{Z_{on}} G_0(0) G_0(Q_j) G_0(2Q_j) \quad (A 9)$$

$$c_j = \int_0^{Z_{on}} G_0(0) G_0(Q_j) G_0(Q_j + Q_j) + G_0(0) G_0(Q_j) G_0(Q_j - Q_j) \quad (A 10)$$

$$d_j = \int_0^{Z_{on}} G_0(0) G_0(Q_j)^2 G_0(2Q_j) + \frac{1}{2} G_0(0)^2 G_0(Q_j)^2 \quad (A 11)$$

$$g_j = \int_0^{Z_{on}} G_0(0)^2 G_0(Q_j) G_0(Q_j) + G_0(0)^2 G_0(Q_j) G_0(Q_j) + G_0(0) G_0(Q_j)^2 G_0(Q_j + Q_j) + G_0(0) G_0(Q_j)^2 G_0(Q_j - Q_j) + 2 G_0(0) G_0(Q_j) G_0(Q_j) G_0(Q_j + Q_j); \quad (A 12)$$

and we have adopted the compactified notation:

$$G_0(q) = G_0(k + q; i!_n) \quad (A 13)$$

$$\int_0^{Z_{on}} \frac{1}{2} \sum_{i!_n} \frac{dk}{(2)^2}; \quad (A 14)$$

As the susceptibility towards ordering is always largest for the fundamental vectors, we integrate out the higher harmonics, which allows us to write the free energy in a form that transparently displays the C_4 symmetry of the problem

$$F = \sum_j r_j (j_{Q_j}^2 + j_{Q_j}^2) + \frac{u_j}{4} (j_{Q_j}^2 + j_{Q_j}^2)^2 + \sum_j j_{Q_j}^2 j_{Q_2}^2; \quad (A 15)$$

The effect of higher harmonics is to renormalize the coefficients of the quartic terms, which become

$$u_j = 4 d_j \quad j_j^2 = r_j \quad j_j = g_j \quad j_j^2 = r_j \quad u_j = 2; \quad (A 16)$$

- ¹ S. A. Kivelson, I. P. Bindloss, E. Fradkin, V. Oganesyan, J. M. Tranquada, A. Kapitulnik, and C. Howard, Rev. Mod. Phys. 75, 1201 (2003).
- ² J. M. Tranquada, H. Woo, T. G. Perring, H. Goka, G. D. Gu, G. Xu, M. Fujita, and K. Yamada, Nature 429, 534 (2004).
- ³ M. P. Lilly, K. B. Cooper, J. P. Eisenstein, L. N. Pfeiffer, and K. W. West, 82, 394 (1999).
- ⁴ J. Robertson, S. A. Kivelson, E. Fradkin, A. Fang, and A. Kapitulnik, cond-mat/0602675.
- ⁵ V. Brouet, W. L. Yang, X. J. Zhou, Z. Hussain, N. Ru,

- K. Y. Shin, I. R. Fisher, and Z. X. Shen, Phys. Rev. Lett. 93, 126405 (2004).
- ⁶ E. D. Masi, M. C. Aronson, J. F. Manseld, B. Foran, and S. Lee, Phys. Rev. B 52, 14516 (1995).
- ⁷ E. D. Masi, B. Foran, M. C. Aronson, and S. Lee, Phys. Rev. B 54, 13587 (1996).
- ⁸ G. H. Gweon, J. D. Denlinger, J. A. Check, J. W. Allen, C. G. Olson, E. D. Masi, M. C. Aronson, B. Foran, and S. Lee, Phys. Rev. Lett. 81, 886 (1998).
- ⁹ H. Komoda, T. Sato, S. Souma, T. Takahashi, Y. Ito, and K. Suzuki, Phys. Rev. B 70, 195101 (2004).

- ¹⁰ H. J. Kim, C. D. Malliakas, A. T. Tomić, S. H. Tessmer, M. G. Kanatzidis, and S. J. L. Billinge, *Phys. Rev. Lett.* **96**, 226401 (2006).
- ¹¹ A. Fang, N. Ru, I. R. Fisher, and A. Kapitulnik, to be published.
- ¹² J. Laverock, S. B. Dugdale, Z. Majr, M. A. Alam, N. Ru, I. R. Fisher, G. Santi, and E. Bruno, *Phys. Rev. B* **71**, 085114 (2005).
- ¹³ Another example of a 2D metal with a unidirectional CDW is the purple bronze Mo_4O_{11} . It is now well known that this material has hidden 1D character related to the presence of conducting chains.^{30,31,32,33} Since there are chains running along three different directions, the system as a whole has hexagonal symmetry. Indeed, the present work was, in part, inspired by the earlier work of Gweon et al, Ref. 33. However, there are no chain-like structural units in RTe_3 .
- ¹⁴ E. Dimasi, B. Foran, M. C. Aronson, and S. Lee, *Chem. Mater.* **6**, 1867 (1994).
- ¹⁵ N. Ru and I. R. Fisher, *Phys. Rev. B* **73**, 033101 (2006).
- ¹⁶ A. Kikuchi, *J. Phys. Soc. Jpn* **67**, 1308 (1998).
- ¹⁷ D. C. Johnston, M. Maki, and G. G. Gruner, *Solid State Commun.* **53**, 5 (1985).
- ¹⁸ R. S. Kwok, G. Gruner, and S. E. Brown, *Phys. Rev. Lett.* **65**, 365 (1990).
- ¹⁹ D. J. Scalapino, Y. Imry, and P. Pincus, *Phys. Rev. B* **11**, 2042 (1975).
- ²⁰ P. A. Lee, T. M. Rice, and P. W. Anderson, *Phys. Rev. Lett.* **31**, 462 (1973).
- ²¹ S. Barisic, in *Electronic properties of inorganic quasi-one-dimensional compounds*, edited by P. Monceau (Elsevier Publishing Company, 1985).
- ²² N. Ru, G. Margulis, K. Y. Shin, M. F. Toney, and I. R. Fisher, *cond-mat/0610319*.
- ²³ S. Girault, A. H. Moudden, and J. P. Pouget, *Phys. Rev. B* **39**, 4430 (1989).
- ²⁴ S. H. Lee, J. M. Tranquada, K. Yamada, D. J. Buttrey, Q. Li, and S. W. Cheong, *Phys. Rev. Lett.* **88**, 126401 (2002).
- ²⁵ S. A. Kivelson, E. Fradkin, and V. J. Emery, *Nature (London)* **393**, 550 (1998).
- ²⁶ There is a small orthorhombicity in the crystal structure, which therefore acts as a weak symmetry breaking field. Thus, rather than domains of different orientation stripes, which might otherwise be expected, stripe order with a single ordering vector (Q_2 , not Q_2) is stabilized.
- ²⁷ The crystal unit cell for RTe_3 is doubled from the simple one of the square lattice.⁵ It is also rotated by 45° . If we denote the lattice spacing between nearest Te atoms by a , which we set to be 1 throughout this work, the reciprocal lattice unit a^* in Ref. 5 is actually equal to $2/a = 2$. Then $Q_{\text{CDW}} = 5a^* = 10$. Rotating back by 45° gives, in the simple unit cell scheme used here, $Q_{\text{CDW}} = (5/\sqrt{2}, 5/\sqrt{2})$.
- ²⁸ S. N. Coppersmith, D. S. Fisher, B. I. Halperin, P. A. Lee, and W. F. Brinkman, *Phys. Rev. B* **25**, 349 (1982).
- ²⁹ A. Sacchetti, L. Degiorgi, T. Giamarchi, N. Ru, and I. R. Fisher, to be published.
- ³⁰ M. H. Whangbo, E. Canadell, P. Foury, and J. P. Pouget, *Science* **252**, 96 (1991).
- ³¹ M. Braden, O. Friedt, Y. Sidis, P. Bourges, M. Minakata, and Y. Maeno, *Phys. Rev. Lett.* **88**, 197002 (2002).
- ³² S. Hill, S. Uji, M. Takashita, C. Terakura, T. Terashima, H. Aoki, J. S. Brooks, Z. Fisk, and J. Sarrao, *Phys. Rev. B* **58**, 10778 (1998).
- ³³ G. H. Gweon, S. K. Mo, J. W. Allen, C. R. Ast, H. Hochst, J. L. Sarrao, and Z. Fisk, *Phys. Rev. B* **72**, 35126 (2005).